

GATraj: A Graph- and Attention-based Multi-Agent Trajectory Prediction Model

Hao Cheng^{1,3*}, Mengmeng Liu^{1*}, Lin Chen², Hellward Broszio², Monika Sester¹, Michael Ying Yang³

Abstract—Trajectory prediction has been a long-standing problem in intelligent systems such as autonomous driving and robot navigation. Recent state-of-the-art models trained on large-scale benchmarks have been pushing the limit of performance rapidly, mainly focusing on improving prediction accuracy. However, those models put less emphasis on efficiency, which is critical for real-time applications. This paper proposes an attention-based graph model named *GATraj* with a much higher prediction speed. Spatial-temporal dynamics of agents, *e.g.*, pedestrians or vehicles, are modeled by attention mechanisms. Interactions among agents are modeled by a graph convolutional network. We also implement a Laplacian mixture decoder to mitigate mode collapse and generate diverse multimodal predictions for each agent. Our model achieves performance on par with the state-of-the-art models at a much higher prediction speed tested on multiple open datasets.

I. INTRODUCTION

Accurately predicting how agents (*e.g.*, pedestrians and vehicles) move in a variety of environments is crucial for many intelligent systems, such as autonomous driving and robot navigation. With accurate prediction of other agents' trajectories in the vicinity, an automated ego agent can safely navigate its own path. However, trajectory prediction is very challenging due to various reasons. First, agents' behaviors are stochastic as they mutually influence each other, such as avoiding collisions or staying closely in a subgroup. Second, the information available to derive an agent's behavior is often limited. The destination at which an agent wants to arrive usually is unknown. The ego agent can only estimate other agents' behaviors based on their past moving dynamics like velocity and heading directions, interactions based on relative positions, and even environmental contextual constraints. Due to the mutual influence among agents and the moving dynamics in both spatial and temporal dimensions, an agent's behavior can be multimodal, *e.g.*, moving into different directions at various speeds. Hence, trajectory prediction needs to consider both spatial-temporal dynamics and multimodalities of agents' behaviors.

As exemplified in Fig. 1, recent deep learning models trained on large-scale real-world datasets have significantly improved trajectory prediction accuracy on multiple benchmarks measured by distance errors. These models address

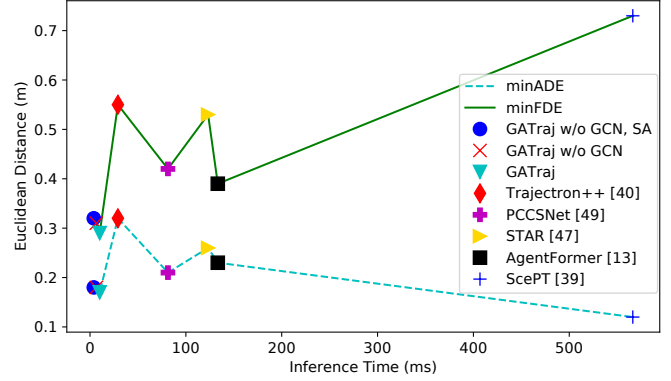


Fig. 1: The inference speed and the prediction performance of the models on the Zara2 dataset [1] computed from a single Tesla V100 GPU. GATraj runs faster than other prediction methods and achieves superior performance. SA: self-attention [2]; GCN: graph convolutional network [3].

the prediction task by utilizing some or all of the following information: (i) The ego agent's past trajectory in lateral and longitudinal coordinates is used as input trajectory. A popular time horizon setting is letting the model observe eight-time steps and predict the next 12-time steps in a 2.5Hz sampling rate for pedestrians on the ETH/UCY benchmark [4], [1], or letting the model observe up to four-time steps and predict the next 12-time steps in a 2 Hz for autonomous driving on the nuScenes benchmark [5]. Other newly released datasets [6], [7] are more challenging with even shorter observation but longer prediction time horizon. (ii) Agent-to-agent interactions are modeled over time and space. A widely used way is to map the neighboring agents onto an occupancy map centralized at the position of the ego agent [8]. Alternatively, connections between agents are modeled via a graphic model [9]. (iii) Environmental contexts are used to constrain an agent's movement. For example, convolutional and attention-based approaches are used to extract contextual information from rasterized data like semantic maps and images [10], or vectorized data like High-Definition (HD) maps [11]. However, map information is not always given in an open environment. Hence, many models still address trajectory prediction without necessarily including map information [12], [13].

Most of the current studies on trajectory prediction have only focused on reducing prediction error, while model efficiency has not yet been treated in much detail as it should be, preventing the usage of complex trajectory prediction models in real-time scenarios. To this end, we propose a graph- and attention-based multi-agent trajectory prediction

*Equal contribution, name in alphabet order

¹Institute of Cartography and Geoinformatics, Leibniz University Hannover, Germany, {cheng, sester}@ikg.uni-hannover.de, mengmeng.liu@stud.uni-hannover.de;

²VISCODA GmbH, Schneiderberg 32, 30167 Hannover, Germany, {chen, broszio}@viscoda.com

³Scene Understanding Group, University of Twente, The Netherlands, michael.yang@utwente.nl

model, *GATraj*. *GATraj* takes into account agents' spatial-temporal dynamics and their multimodal trajectories in the prediction time, with the model's efficiency at a fast prediction speed. Our model adopts attention mechanisms [2] to learn agents' spatial-temporal dynamics. Agent-to-agent interaction is modeled by a graph convolutional network (GCN) based module using message passing [3]. In the end, a Laplacian mixture decoder predicts diverse multimodal trajectories for each agent. In this work, we do not consider any environmental contextual information for a more applicable setting. The **main contributions** of our work are as follows:

- We propose an end-to-end multimodal trajectory prediction model with a Laplacian Mixture Density Network (MDN) decoder and winner-takes-all [14] loss function to mitigate the mode collapse problem and generate diverse predictions.
- We provide a GCN module to learn agent-to-agent interactions and an attention module to extract spatial-temporal dynamics.
- *GATraj* achieves performance on par with the state-of-the-art models at a much higher prediction speed tested on multiple datasets.

II. RELATED WORK

Many early works, *e.g.*, [15], [16], [17], rely on hand-crafted features to model agents' movements. Among them, Social Force Models (SFMs) [16] are the most influential ones, which apply different forces to determine agents' speed and orientation, such as repulsive force for collision avoidance with obstacles and attractive force for social connections among agents and goals. Trajectory prediction is also widely modeled by *e.g.*, cellular automaton [18], Kalman filter [15], Gaussian process [19], Markov Models [17], and game theoretic models [20]. Given the complex dynamics in both spatial and temporal domains, these models based on manually selected or designed features often have limited performance for modeling multi-agent interactions and their multimodalities of potential future trajectories.

In recent years, data-driven models with an encoder-decoder structure have dominated model designs on trajectory prediction. The pioneering work Social-LSTM [8] explores Long Short-Term Memories (LSTMs) [21] to encode pedestrians' motion dynamics into the so-called hidden states and a pooling mechanism to model interactions. Many later works [22], [12] extend this structure by including more features, such as agent-to-agent and agent-to-environment interactions using LSTM or other Recurrent Neural Network variants, *e.g.*, Gated Recurrent Units (GRUs) [23]. However, the model performances highly depend on the hidden states of the encoder-decoder structure. With the increase in trajectory length and complexity, the performances are often heavily degraded [24].

Attention-based auto-regression models [2] and graph models GCNs [3] are leveraged to tackle long time-dependency and complex connectivity problems in trajectory prediction. Recently, the self- and cross-attention mechanisms [2] have shown their effectiveness in learning complex

spatial-temporal interconnections. They achieve state-of-the-art performance on various trajectory prediction benchmarks [25], [26], [27], [28]. For example, AgentFormer [13] proposes an agent-aware attention mechanism that simultaneously models the time and social dimensions among agents. In addition to the attention mechanisms, GCNs are widely used to model interactions [9], [29], [30]. Agents are denoted as nodes, and their connections are denoted as edges. This way, the interactions between agents are learned via message passing through the nodes. In this paper, an implementation of the attention mechanisms to learn salient spatial-temporal features and a GCN module to model agent-to-agent interactions is described.

In order to predict multiple feasible future trajectories, deep generative models are applied. The most commonly adopted model designs are, *e.g.*, Generative Adversarial Nets (GANs), Variational Auto-Encoder [31] as well as its extension Conditional-VAE (CVAE) [32], and Normalizing Flows [33]. The representative trajectory prediction frameworks applying these designs are, *e.g.*, Social-GAN [34], DESIRE [35], and Precog [36], respectively. Due to the relatively easy training process and good performance, many recent works [37], [13], [38], [39] extend the CVAE-based design for multimodal trajectory prediction. However, these sampling-based approaches do not provide a straightforward mechanism to estimate the likelihood of each prediction in the random sampling process. Hence, apart from deep generative models, MDNs are proposed to learn a mixture density function, such as Gaussian Mixture Model (GMM), for multimodal trajectory prediction [40], [29], [41], [42]. Nevertheless, most benchmarks only provide a single ground truth trajectory for supervising the learning process. Those models often cannot learn the entire data distribution and generate diverse predictions, which is referred to as the so-called mode collapse problem [43].

The previously mentioned methods inspire the design of our model. *GATraj* adopts an encoder-decoder structure to encode the observed information, *i.e.*, past trajectories and interactions, for predicting future trajectories. Spatial-temporal features are extracted by attention mechanisms, and a GCN models interactions among agents. Instead of using a GMM, a Laplacian mixture decoder to generate multiple diverse predictions for each agent is presented.

III. METHODOLOGY

A. Problem Formulation

A multi-path trajectory prediction problem is defined as predicting a set of future trajectories $\{\hat{\mathbf{Y}}_{i,1}^{T+1:T+T'}, \hat{\mathbf{Y}}_{i,2}^{T+1:T+T'}, \dots, \hat{\mathbf{Y}}_{i,K}^{T+1:T+T'}\}$ given the observed trajectory $\mathbf{X}_i^{1:T} = \{X_i^1, X_i^2, \dots, X_i^T\}$ of agent i . Here, T and T' denote the total time steps of the observed trajectory and the set of predicted trajectories, respectively; $T + T'$ is the total sequence length. K stands for the number of the modes of multiple predicted trajectories. $X_i^t = \{x_i^t, y_i^t\} \in \mathbb{R}^2$ is the position of agent i at time step t in a 2D coordinate system. The formulation can also be easily extended to a 3D coordinate system. To simplify the notation, \mathbf{X} and \mathbf{Y} denote

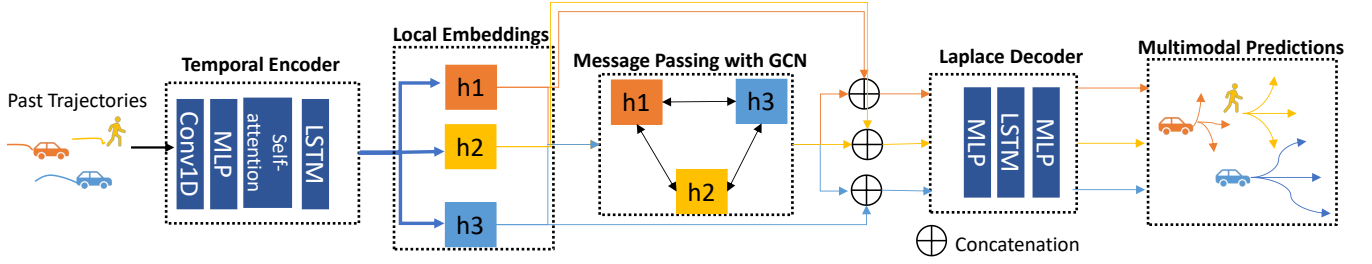


Fig. 2: The framework of the proposed model GATraj.

the observed and ground truth trajectories, respectively. We aim to reduce the distance between a predicted trajectory $\hat{\mathbf{Y}}$ and the corresponding ground truth trajectory \mathbf{Y} for all agents.

Translation invariant representation of the input trajectories is carried out before feeding the trajectory data into the prediction model. We follow [37] to use relative positions instead of absolute positions to mitigate domain gaps across different scenes. First, we shift the origin to each agent's last observed time step for data normalization. Then, we use $\Delta\mathbf{X}_i^{2:T} = \{\Delta X_i^2, \Delta X_i^3, \dots, \Delta X_i^T\}$ to represent agent i 's observed trajectory, where $\Delta X_i^t = \{\Delta x_i^t, \Delta y_i^t\}$ is the offset from $(t-1)$ to the next time step. However, this translation-invariant representation of trajectories also loses the relative position information between agents, which is essential for modeling their interactions. Hence, we obtain the relative position between agent i and j based on their original positions $(x_i^t - x_j^t, y_i^t - y_j^t)$ at each time step, where $i \neq j$. The relative position is further employed in the global interaction.

B. The Proposed Framework

Figure 2 depicts the overview of our proposed framework GATraj. It consists of three parts: a Temporal Encoder, a GCN-based global interaction module, and a Laplacian Decoder. We first utilize the encoder to extract temporal information of each agent independently and output rich temporal information for the subsequent modules. Then the global interaction module, which employs a GCN adopted from [9], aggregates the temporal context of different agents over time and space and updates each agent's hidden state by message passing for interaction modeling. Finally, the learned spatial-temporal feature map is the input of the Laplacian decoder that simultaneously predicts diverse and multimodal future trajectories for all the agents. We explain each part of GATraj in detail in the following.

a) Temporal Encoder: The self-attention Temporal Encoder learns temporal dynamic information from the observed trajectory. It takes as input the relative positions $\Delta\mathbf{X}_i^{2:T}$, which is later passed to a 1D convolution layer (Conv1D) and a 2-layer position-wise multilayer perceptron (MLP). Then we employ three Transformer Encoder blocks [2] to learn salient temporal features - to which time steps of the temporal sequence the encoder should pay more attention through the self-attention layer. Specifically, the default positional encodings of the Transformer network are added at the bottom of the encoder blocks to retain the

ordered sequential information. After that, a multi-head of self-attention is applied to jointly attend to the information from different representation subspaces at different positions. Eight heads of self-attention and skip-connections are used in our implementation. Towards the end of the temporal encoder, we utilize an LSTM to extract the temporal dependencies over time. Note that each ego agent's observed trajectory is considered independently so that their temporal dynamics are processed in parallel.

b) Global Interaction: We build a GCN-based module adopted from SR-LSTM [9] for modeling global interactions among all the concurrent agents in a given scene. Original SR-LSTM introduces a States Refinement (SR) module to refine the cell state of an LSTM by passing messages among agents at each time step. In contrast, to reduce the computational cost, GATraj only refines cell state once at the latest observed time step but still maintains the ability to model interactions among agents. More specifically, we follow SR-LSTM to use the motion gate and agent-wise attention to preserve spatial relationships between the ego agent and its neighbors and to select the most helpful information from neighboring agents for message passing. The cell state output by the LSTM in the Temporal Encoder is updated by a social-aware information selection mechanism as follows:

$$\hat{c}_i^{T,l+1} = \phi_{\text{mp}} \left[\sum_{j \in N(i)} \alpha_{i,j}^{T,l} (g_{i,j}^{T,l} \odot \hat{h}_j^{T,l}) \right] + \hat{c}_i^{T,l}, \quad (1)$$

where \hat{c}_i denotes agent i 's cell state after message passing, l denotes the message passing times, \odot is the element-wise product operation, and ϕ_{mp} denotes an MLP. Namely, for the ego agent i , the cell state starts at $l=0$ with the original output of LSTM c_i . All the LSTM hidden states $\hat{h}_j^{T,l}$ of its neighbors $j \in N(i)$ are aggregated through the motion gate $g_{i,j}^{T,l}$, and the agent-wise attention $\alpha_{i,j}$ attends to the neighbors based on the agent-to-agent pairwise weights. In addition, a skip connection adds agent i 's previously refined cell $\hat{c}_i^{T,l}$. Here, the motion gate is defined by using the relative position between agent i and j , and their individual hidden states, as shown in Eq. (2) and (3),

$$r_{i,j}^{T,l} = \phi_r(x_i^T - x_j^T, y_i^T - y_j^T), \quad (2)$$

$$g_{i,j}^{T,l} = \delta(\phi_m[r_{i,j}^{T,l}, \hat{h}_j^{T,l}, \hat{h}_i^{T,l}]), \quad (3)$$

where ϕ_m and ϕ_r denote MLP and δ is the Sigmoid function.

Similarly, another MLP ϕ_a is used to learn the weights $u_{i,j}^{T,l}$ of the different impacts from the neighbors by Eq. (4). The weights are normalized across all the neighboring agents

using the Softmax function denoted by Eq. (5),

$$u_{i,j}^{T,l} = \phi_a[r_{i,j}^{T,l}, \hat{h}_j^{T,l}, \hat{h}_i^{T,l}], \quad (4)$$

$$\alpha_{i,j}^{T,l} = \frac{\exp(u_{i,j}^{T,l})}{\sum_{s \in N(i)} \exp(u_{i,s}^{T,l})}. \quad (5)$$

The hidden state of the ego agent i then is updated using Eq. (6) after the cell state $\hat{c}_i^{T,l+1}$ is refined by the above message passing.

$$\hat{h}_i^{T,l+1} = \hat{h}_i^{T,l} + \tanh(\hat{c}_i^{T,l+1}), \quad (6)$$

where \tanh stands for the hyperbolic tangent function. Different from SR-LSTM, we use a skip-connection to avoid the vanishing gradient problem and discard the output gate from the SR-LSTM original implementation inspired by the LSTM gate structure. Compared to the original GCNs [3] that use adjacency matrix to compute normalization constant, this agent-wise attention uses learnable MLP ϕ_r and ϕ_a to aggregate relative spatial positional information between the ego and all its neighboring agents and emphasize important neighbors using the attention mechanism to guide the message passing.

c) **Laplacian Decoder:** We introduce a Laplacian MDN decoder to generate future multimodal trajectories. The decoder takes as input the spatial-temporal dynamic context from the encoder and the GCN module. Its outputs are a set of different modes of the predicted trajectory distribution $\sum_{k=1}^K \pi_k \text{Laplace}(\mu, b)$. Here, π_k represents the probability of each mode and $\sum_{k=1}^K \pi_k = 1$. μ and b stand for each Laplace component's location and scale parameter. Concretely, the decoder takes as input the hidden state h_i^T of the LSTM from the Temporal Encoder and the hidden state $\hat{h}_i^{T,l+1}$ and cell state $\hat{c}_i^{T,l+1}$ after the message passing with the GCN module. Here, $\{h_i^T, \hat{h}_i^{T,l+1}, \hat{c}_i^{T,l+1}\} \in \mathbb{R}^{N \times D}$, where D is the dimension of the embedded feature space and N is the total number of agents in the current scene. First, an MLP projects the shape of the input into $[K, N, D]$, where K is the number of modes to be predicted. With projected feature embeddings, we utilize an MLP and a Softmax function to learn the probability $\hat{\pi}_{i,1:K}$ of each mode for each agent. Then, an LSTM decodes the aggregated and embedded hidden states into a shape of $[K \times N, T', D]$, recovering the prediction time-step dimension T' . We empirically found that using LSTM contributes to a more efficient gating of the sequential information over the time axis (more details in Sec. IV-E). Finally, two side-by-side MLPs predicts a mixture of Laplace distribution with K modes of the potential future trajectories for each agent, *i.e.*, the location $\hat{\mathbf{Y}}_{i,1:K} \in \mathbb{R}^{K \times T' \times 2}$ and its associated scale $\hat{\mathbf{b}}_{i,1:K} \in \mathbb{R}^{K \times T' \times 2}$, and $\hat{\pi}_{i,1:K} \in \mathbb{R}^K$. It should be noted that we directly use the location of the Laplace distribution as the predicted trajectory for each agent.

C. Loss Function

The total loss of GATraj is decoupled into two parts - *regression loss* and *classification loss*. We utilize a Winner-Takes-All strategy [14] for the supervision by each agent's single ground truth trajectory to encourage GATraj to generate diverse predictions. Namely, for the regression loss, we

only optimize the best mode k^* of the K predictions during training instead of the weighted strategy by an Expectation-Maximization algorithm for a GMM. Following [27], we employ the negative log-likelihood for the Laplace distribution as the regression loss and the cross-entropy loss as the classification loss for the mode optimization,

$$k^* = \arg \min_{k \in K} \|\hat{\mathbf{Y}}_{i,k} - \mathbf{Y}_i\|^2, \quad (7)$$

$$\mathcal{L}_{\text{reg},i} = \frac{1}{T'} \sum_{t=T+1}^{T+T'} -\log P(\mathbf{Y}_i^t | \hat{\mathbf{Y}}_{i,k^*}^t, \mathbf{b}_{i,k^*}^t), \quad (8)$$

$$\mathcal{L}_{\text{cls},i} = \sum_{k=1}^K -\pi_{i,k} \log(\hat{\pi}_{i,k}), \quad (9)$$

where $\log P(\cdot | \cdot)$ is the logarithmic probability density function of the Laplace distribution. $\hat{\pi}_{i,k}$ is the predicted probability, and $\pi_{i,k}$ is our target probability. We employ a soft displacement error adopted from [27] as our target probability.

IV. EXPERIMENTS

A. Dataset

The benchmarks ETH/UCY [4], [1] and nuScenes [5] are used to train and test the performance of our proposed model. ETH/UCY contains thousands of pedestrian trajectories sampled in 2.5 Hz in five different subsets, *i.e.*, Eth, Hotel, Uni, Zara1, and Zara2. The time horizon lets the model observe eight steps and predict the subsequent 12-step trajectories. We follow the standard leave-one-out training and test partitioning - four of the five subsets are used for training, and the left-out one is for the test. This partitioning is iterated for each subset. nuScenes prediction task provides separate training and test sets for vehicle trajectory prediction. A trajectory is sampled in 2 Hz. The model observes up to four-time steps and predicts the following 12-step trajectories. We use the provided data partitioning for training and testing.

B. Evaluation Metrics and Baselines

We apply the two most commonly used metrics, Average Displacement Error (ADE) and Final Displacement Error (FDE) in meters, to evaluate trajectory prediction accuracy. ADE measures the Euclidean distance between the predicted and ground truth trajectories and is averaged at each position for each agent. FDE is the Euclidean distance of the last position between the predicted and ground truth trajectories.

$$\text{ADE}_K = \frac{1}{N} \frac{1}{T'} \min_{k=1}^K \sum_{i=1}^N \sum_{t=T+1}^{T+T'} \|\hat{\mathbf{y}}_{i,k}^t - \mathbf{y}_i^t\|^2, \quad (10)$$

$$\text{FDE}_K = \frac{1}{N} \min_{k=1}^K \sum_{i=1}^N \|\hat{\mathbf{y}}_{i,k}^{T+T'} - \mathbf{y}_i^{T+T'}\|^2, \quad (11)$$

where N is the total number of agents. Here, K denotes that we generate K predictions for each agent and report the best one measured by ADE and FDE, respectively.

To make a fair comparison, we only benchmark our model GATraj with multi-path trajectory prediction models. Namely, they are convolutional based multi-path trajectory

prediction models CoverNet [5] and MTP [44]; GAN-based model Social-GAN [34]; CVAE-based models DLow-AF [45] and ScePT [39]; Normalizing flow-based model LDS-AF [46]; GCN-based models STAR [47]; GMM-based models MultiPath [48] and Trajectron++ [40]; attention-based models SoPhie [10], AgentFormer [13], MID [26]; clustering-based model PCCSNet [49]; belief energy-based model LB-EBM [50]. It should be noted that some of the baseline models [10], [44], [48] also include scene information. But our model is only trained on the trajectory data.

C. Experimental Setting

The hyper-parameters of GATraj are as follows. The hidden states and the embedding dimensions are all set to 64. We apply the Adam optimizer [51] with a learning rate of $5e^{-4}$ and a cosine annealing schedule until it reaches $1e^{-5}$. The batch size is set to 32, and the maximum epoch is set to 1000. On ETH/UCY, the maximum distance of the ego and neighboring agents is set to 10m and the messaging passing time $l = 2$, which are the same settings as in SR-LSTM. On nuScenes, given the faster driving speed of vehicles and fewer neighboring agents than ETH/UCY, the maximum distance of the ego and neighboring agents is set to 100m and the messaging passing time $l = 1$. All our models are trained on Google Colab with a single Tesla P100 GPU. Our code will be released at <https://github.com/mengmengliu1998/GATraj> with detailed settings.

D. Results

Table I and II present the evaluation performance on the nuScenes and ETH/UCY benchmarks, respectively. Compared to the other models, except AgentFormer with map information, our model achieves the best performance measured by ADE and FDE in predicting 5 and 10 trajectories for each agent. The performance of our model trained merely using trajectory data only slightly falls behind AgentFormer with extra map information. Our model achieves performance on par with the state-of-the-art model ScePT on the ETH/UCY benchmark for predicting 20 trajectories for each agent. In contrast, ScePT uses a conditional policy learning to decode scene-consistent predictions but yields higher FDE. Due to the auto-regressive policy net and the partitioning of the scene-graph into cliques, ScePT also requires longer computational time (see Table III).

TABLE I: Quantitative results on nuScenes [5]. The best/2nd best performances are indicated in boldface and underline.

Model	Map info.	ADE ₅	FDE ₅	ADE ₁₀	FDE ₁₀
MTP [44]	Yes	2.93	-	2.93	-
MultiPath [48]	Yes	2.32	-	1.96	-
DLow-AF [45]	No	2.11	4.70	1.78	3.58
LDS-AF [46]	No	2.06	4.62	1.65	3.50
AgentFormer [13]	No	1.97	4.21	1.58	3.14
CoverNet baseline [5]	Yes	1.96	-	1.48	-
Trajectron++ [40]	Yes	1.88	-	1.51	-
AgentFormer [13]	Yes	1.86	3.89	1.45	2.86
Ours	No	<u>1.87</u>	<u>4.08</u>	<u>1.46</u>	<u>2.97</u>

TABLE II: Quantitative results on ETH/UCY [4], [1] measured by ADE₂₀/FDE₂₀. The best performance is in boldface.

Models	Eth	Hotel	Uni	Zara1	Zara2	Avg.
Social-GAN[34]	0.81/1.52	0.72/1.61	0.60/1.26	0.34/0.69	0.42/0.84	0.58/1.18
SoPhie [10]	0.70/1.43	0.76/1.67	0.54/1.24	0.30/0.63	0.38/0.78	0.54/1.15
Trajectron++[40]	0.67/1.18	0.18/0.28	0.30/0.54	0.25/0.41	0.18/0.32	0.32/0.55
STAR [47]	0.36/0.65	0.17/0.36	0.31/0.62	0.26/0.55	0.22/0.46	0.26/0.53
AgentFormer[13]	0.45/0.75	0.14/0.22	0.25/0.45	0.18/0.30	0.14/0.24	0.23/0.39
MID [26]	0.39/0.66	0.13/0.22	0.22/0.45	0.17/0.30	0.13/0.27	0.21/0.38
LB-EBM [50]	0.30/0.52	0.13/0.20	0.27/0.52	0.20/0.37	0.15/0.29	0.21/0.38
PCCSNet [49]	0.28/0.54	0.11/0.19	0.29/0.60	0.21/0.44	0.15/0.34	0.21/0.42
ScePT [39]	0.10/0.65	0.13/0.77	0.12/0.65	0.13/0.77	0.14/0.81	0.12/0.73
Ours	0.26/ 0.42	0.10/0.15	0.21/ 0.38	0.16/ 0.28	0.12/0.21	0.17/ 0.29

* The results of Trajectron++ and AgentFormer are updated according to implementation issue #53 [52] and issue #5 [53], respectively. Based on the published implementation, except the model underlined (SoPhie), all the other models do not use scene information on the ETH/UCY dataset.

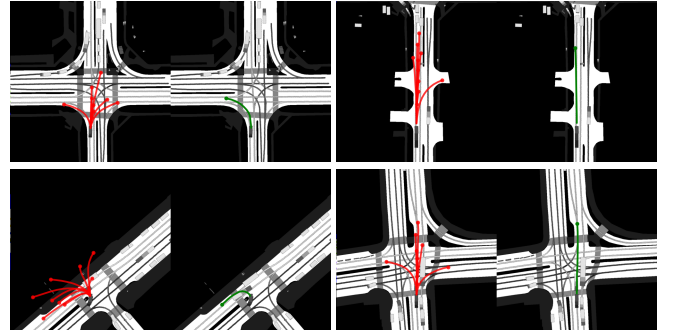


Fig. 3: Qualitative results of GATraj on nuScenes [5]. The observed trajectory is denoted as dark rectangles with descending grayscale along the time steps, the prediction is in red dotted lines, and the corresponding ground truth is in green dotted lines. The HD map is only used for visualization and not used as extra contextual information for prediction.

Figure 3 shows the qualitative results on nuScenes. GATraj generates diverse multimodal predictions for the ego agent, such as turning into different directions (upper left and lower right subfigures), moving at different speeds (upper right subfigure), and even making a U-turn (lower left subfigure). However, even though at least one of the multiple predicted trajectories is very close to the corresponding ground truth trajectory, some modes of the predictions are inconsistent with the lanes or unfeasible in terms of the scene constraints. It is extremely challenging for the model to achieve scene-consistent prediction without knowing the scene information.

Figure 1 and Table III show the comparison of the model size and the prediction speed between our model and the models with similar prediction performance. We conduct this experiment on Zara2 [1] using a single Tesla V100 GPU and a batch size of 32. Our full model demonstrates an almost three-fold faster prediction speed (*i.e.*, 10.1 ms vs. 29.1 ms) than the 2nd fastest model Trajectron++. By removing the GCN-based interaction module and the attention mechanisms, our model can reach a speed of 3.9 ms, and the size of our model is also decreased from 276 K to 183 K. Even without the GCN and attention mechanisms, our model maintains a relatively good prediction accuracy, as shown in Table IV and V.

TABLE III: Model Efficiency in terms of number of parameters and inference speed on the Zara2 dataset [1]. The best performance is in boldface.

Models	# Params (K)	Speed (ms)
STAR [47]	965	123.2
Trajectron++ [40]	126	29.1
AgentFormer [13]	592	133.3
PCCSNet [49]	347	81.3
ScePT [39]	139	566.3
Ours w/o GCN	259	6.6
Ours w/o GCN, SA	183	3.9
Proposed model	276	10.1

E. Ablation Studies

We conduct a series of ablation studies to analyze the effectiveness of the input information, the self-attention mechanisms, the GCN module, the choice of decoded distribution, and the layer of the decoder. Table IV and V show the performance differences tested on nuScenes and ETH/UCY, respectively. Our model using offset sequences achieves better performance than position or both as the trajectory input on ETH/UCY, but similar performance on nuScenes. Interestingly, using both position and offset as input does not reduce the prediction errors on nuScenes. The effectiveness of the self-attention mechanisms is not so obvious on nuScenes, while the model’s performance decreases without the self-attention mechanisms on ETH/UCY. The reason could be that nuScenes only lets the model observe a short trajectory, *i.e.*, from two to four-time steps, while ETH/UCY provides eight-time steps for observation; The self-attention mechanisms may work better on longer sequences. After removing the GCN module, the performance drops clearly on both datasets. Also, the performance decreases when we substitute the Laplacian MDN with a GMM MDN decoder. Moreover, replacing the LSTM layer with an MLP in the decoder leads to an apparent decrease in performance. Our full model with the proposed modules generally achieves the best performance compared to other ablative models.

TABLE IV: Ablation study on nuScenes [5]. SA denotes the self-attention module. IN denotes using offset (O), position (P), or both (B) as the input data. LMM and GMM represent that the decoder’s outputs are Gaussian (e.g., mean and standard deviation) or Laplace parameters (e.g., location and scale). MLP and LSTM denote that the decoder uses LSTM or MLP to aggregate the sequential information. The best performance is in boldface.

IN	Modules							Performance			
	SA	GCN	GMM	LMM	MLP	LSTM		ADE_5	FDE_5	ADE_{10}	FDE_{10}
O	✓	-	-	✓	-	✓		2.00	4.46	1.57	3.28
O	-	-	-	✓	-	✓		2.00	4.45	1.57	3.29
O	✓	-	✓	-	-	✓		2.08	4.67	1.64	3.45
O	✓	-	-	✓	✓	-		2.03	4.51	1.58	3.28
P	✓	✓	-	✓	-	✓		1.86	4.05	1.48	3.00
B	✓	-	-	✓	-	✓		2.00	4.46	1.58	3.31
O	✓	✓	-	✓	-	✓		1.87	4.08	1.46	2.97

We carry out an additional ablation study to further

TABLE V: Ablation study on the ETH/UCY dataset [4], [1]. The best performance is in boldface.

Models\Datasets	Eth	Hotel	Uni	Zara1	Zara2	Avg.
w/o SA	0.29/0.49	0.11/0.17	0.22/0.40	0.17/0.32	0.12/0.22	0.18/0.32
w/o GCN	0.29/0.45	0.10/0.15	0.21/0.40	0.17/0.32	0.12/0.22	0.18/0.31
GMM loss	0.27/0.47	0.11/0.18	0.22/0.40	0.18/0.34	0.12/0.23	0.18/0.32
MLP Decoder	0.27/0.43	0.11/0.16	0.21/0.39	0.17/0.31	0.12/0.22	0.18/0.30
w/ P input	0.29/0.44	0.12/0.17	0.22/0.40	0.18/0.33	0.12/0.22	0.19/0.31
w/ P & O input	0.28/0.44	0.11/0.16	0.22/0.40	0.18/0.33	0.12/0.22	0.18/0.31
Proposed model	0.26/0.42	0.10/0.15	0.21/0.38	0.16/0.28	0.12/0.21	0.17/0.29

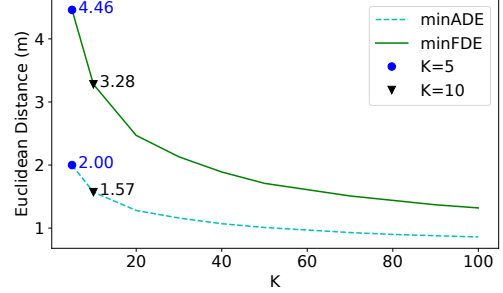


Fig. 4: The prediction results on nuScenes [5] with increasing the number of components in the Laplacian MDN decoder. GATraj w/o GCN achieves 2.00/4.46 of ADE_5/FDE_5 and 1.57/3.28 of ADE_{10}/FDE_{10} , respectively.

analyze the performance of the Laplacian MDN decoder by increasing the number of components. The results shown in Fig. 4 demonstrate that increasing the number of components of the MDN decoder evidently leads to a gain in prediction accuracy. This trend indicates that the Laplacian MDN decoder can generate diverse multimodal predictions. However, many benchmarks limit the maximum number of predictions for each agent, *i.e.*, ETH/UCY recommends 20, and nuScene only allows up to ten predictions for each agent. The limited computational resources of real-time applications may only allow a small number of predictions as well. This finding and constraint motivate us to work on aggregation strategies to effectively pool out the best prediction and reduce the unfeasible modes as shown in Fig. 3 of multimodal predictions.

V. CONCLUSION

This paper proposes an attention-based graph model named GATraj for multi-agent trajectory prediction. We use attention mechanisms to learn spatial-temporal dynamics of agents like pedestrians and vehicles and a graph convolutional network to learn interactions among them. A Laplacian mixture density network decoder predicts diverse and multimodal trajectories for each agent. GATraj achieves performance on par with the state-of-the-art models at a much higher prediction speed tested on the nuScenes and ETH/UCY benchmarks.

Limitations and future work. Our model does not leverage scene information and has limited performance in achieving scene-consistent prediction. In future work, we will explore strategies to incorporate scene information and reduce unfeasible modes of multimodal predictions.

REFERENCES

- [1] A. Lerner, Y. Chrysanthou, and D. Lischinski, "Crowds by example," in *Computer graphics forum*, vol. 26, no. 3. Wiley Online Library, 2007, pp. 655–664.
- [2] A. Vaswani, N. Shazeer, N. Parmar, J. Uszkoreit, L. Jones, A. N. Gomez, Ł. Kaiser, and I. Polosukhin, "Attention is all you need," in *NeurIPS*, 2017, pp. 5998–6008.
- [3] M. Welling and T. N. Kipf, "Semi-supervised classification with graph convolutional networks," in *International Conference on Learning Representations (ICLR)*, 2017.
- [4] S. Pellegrini, A. Ess, K. Schindler, and L. Van Gool, "You'll never walk alone: Modeling social behavior for multi-target tracking," in *2009 IEEE 12th international conference on computer vision*. IEEE, 2009, pp. 261–268.
- [5] H. Caesar, V. Bankiti, A. H. Lang, S. Vora, V. E. Liong, Q. Xu, A. Krishnan, Y. Pan, G. Baldan, and O. Beijbom, "nuscenes: A multimodal dataset for autonomous driving," in *CVPR*, 2020.
- [6] P. Sun, H. Kretschmar, X. Dotiwalla, A. Chouard, V. Patnaik, P. Tsui, J. Guo, Y. Zhou, Y. Chai, B. Caine *et al.*, "Scalability in perception for autonomous driving: Waymo open dataset," in *Proceedings of the IEEE/CVF conference on computer vision and pattern recognition*, 2020, pp. 2446–2454.
- [7] B. Wilson, W. Qi, T. Agarwal, J. Lambert, J. Singh, S. Khandelwal, B. Pan, R. Kumar, A. Hartnett, J. K. Pontes *et al.*, "Argoverse 2: Next generation datasets for self-driving perception and forecasting," in *Thirty-fifth Conference on Neural Information Processing Systems Datasets and Benchmarks Track (Round 2)*, 2021.
- [8] A. Alahi, K. Goel, V. Ramanathan, A. Robicquet, L. Fei-Fei, and S. Savarese, "Social lstm: Human trajectory prediction in crowded spaces," in *Proceedings of the IEEE conference on computer vision and pattern recognition*, 2016, pp. 961–971.
- [9] P. Zhang, W. Ouyang, P. Zhang, J. Xue, and N. Zheng, "Sr-lstm: State refinement for lstm towards pedestrian trajectory prediction," in *Proceedings of the IEEE/CVF Conference on Computer Vision and Pattern Recognition*, 2019, pp. 12 085–12 094.
- [10] A. Sadeghian, V. Kosaraju, A. Sadeghian, N. Hirose, H. Rezatofighi, and S. Savarese, "Sophie: An attentive gan for predicting paths compliant to social and physical constraints," in *Proceedings of the IEEE/CVF conference on computer vision and pattern recognition*, 2019, pp. 1349–1358.
- [11] J. Gu, C. Sun, and H. Zhao, "Densetnt: End-to-end trajectory prediction from dense goal sets," in *Proceedings of the IEEE/CVF International Conference on Computer Vision*, 2021, pp. 15 303–15 312.
- [12] H. Cheng, W. Liao, M. Y. Yang, B. Rosenhahn, and M. Sester, "Amenet: Attentive maps encoder network for trajectory prediction," *ISPRS Journal of Photogrammetry and Remote Sensing*, vol. 172, pp. 253–266, 2021.
- [13] Y. Yuan, X. Weng, Y. Ou, and K. M. Kitani, "Agentformer: Agent-aware transformers for socio-temporal multi-agent forecasting," in *Proceedings of the IEEE/CVF International Conference on Computer Vision*, 2021, pp. 9813–9823.
- [14] O. Makansi, E. Ilg, O. Cicek, and T. Brox, "Overcoming limitations of mixture density networks: A sampling and fitting framework for multimodal future prediction," in *Proceedings of the IEEE/CVF Conference on Computer Vision and Pattern Recognition*, 2019, pp. 7144–7153.
- [15] R. E. Kalman, "A new approach to linear filtering and prediction problems," *Transactions of the ASME—Journal of Basic Engineering*, vol. 82, no. Series D, pp. 35–45, 1960.
- [16] D. Helbing and P. Molnar, "Social force model for pedestrian dynamics," *Physical review E*, vol. 51, no. 5, p. 4282, 1995.
- [17] K. M. Kitani, B. D. Ziebart, J. A. Bagnell, and M. Hebert, "Activity forecasting," in *European conference on computer vision*. Springer, 2012, pp. 201–214.
- [18] C. Burstedde, K. Klauck, A. Schadschneider, and J. Zittartz, "Simulation of pedestrian dynamics using a two-dimensional cellular automaton," *Physica A: Statistical Mechanics and its Applications*, vol. 295, no. 3–4, pp. 507–525, 2001.
- [19] K. Kim, D. Lee, and I. Essa, "Gaussian process regression flow for analysis of motion trajectories," in *2011 International Conference on Computer Vision*. IEEE, 2011, pp. 1164–1171.
- [20] F. T. Johora, D. Yang, J. P. Müller, and Ü. Özgüner, "On the generalizability of motion models for road users in heterogeneous shared traffic spaces," *IEEE Transactions on Intelligent Transportation Systems*, 2022.
- [21] S. Hochreiter and J. Schmidhuber, "Long short-term memory," *Neural computation*, vol. 9, no. 8, pp. 1735–1780, 1997.
- [22] H. Xue, D. Q. Huynh, and M. Reynolds, "Ss-lstm: A hierarchical lstm model for pedestrian trajectory prediction," in *WACV*, 2018, pp. 1186–1194.
- [23] K. Cho, B. Van Merriënboer, D. Bahdanau, and Y. Bengio, "On the properties of neural machine translation: Encoder-decoder approaches," in *Eighth Workshop on Syntax, Semantics and Structure in Statistical Translation (SSST-8)*, 2014.
- [24] R. Hug, S. Becker, W. Hübner, and M. Arens, "Quantifying the complexity of standard benchmarking datasets for long-term human trajectory prediction," *IEEE Access*, vol. 9, pp. 77 693–77 704, 2021.
- [25] Y. Liu, J. Zhang, L. Fang, Q. Jiang, and B. Zhou, "Multimodal motion prediction with stacked transformers," in *Proceedings of the IEEE/CVF Conference on Computer Vision and Pattern Recognition*, 2021, pp. 7577–7586.
- [26] T. Gu, G. Chen, J. Li, C. Lin, Y. Rao, J. Zhou, and J. Lu, "Stochastic trajectory prediction via motion indeterminacy diffusion," in *Proceedings of the IEEE/CVF Conference on Computer Vision and Pattern Recognition*, 2022, pp. 17 113–17 122.
- [27] Z. Zhou, L. Ye, J. Wang, K. Wu, and K. Lu, "Hivt: Hierarchical vector transformer for multi-agent motion prediction," in *Proceedings of the IEEE/CVF Conference on Computer Vision and Pattern Recognition*, 2022, pp. 8823–8833.
- [28] J. Ngiam, V. Vasudevan, B. Caine, Z. Zhang, H.-T. L. Chiang, J. Ling, R. Roelofs, A. Bewley, C. Liu, A. Venugopal, D. J. Weiss, B. Sapp, Z. Chen, and J. Shlens, "Scene transformer: A unified architecture for predicting future trajectories of multiple agents," in *International Conference on Learning Representations (ICLR)*, 2022.
- [29] X. Shi, X. Shao, Z. Fan, R. Jiang, H. Zhang, Z. Guo, G. Wu, W. Yuan, and R. Shibasaki, "Multimodal interaction-aware trajectory prediction in crowded space," in *Proceedings of the AAAI Conference on Artificial Intelligence*, vol. 34, no. 07, 2020, pp. 11 982–11 989.
- [30] T. Gilles, S. Sabatini, D. Tsishkou, B. Stanculescu, and F. Moutarde, "Gohome: Graph-oriented heatmap output for future motion estimation," in *2022 International Conference on Robotics and Automation (ICRA)*. IEEE, 2022, pp. 9107–9114.
- [31] D. P. Kingma and M. Welling, "Auto-encoding variational bayes," in *International Conference on Learning Representations (ICLR)*, 2014.
- [32] D. P. Kingma, S. Mohamed, D. Jimenez Rezende, and M. Welling, "Semi-supervised learning with deep generative models," *Advances in neural information processing systems*, vol. 27, 2014.
- [33] D. Rezende and S. Mohamed, "Variational inference with normalizing flows," in *International conference on machine learning*. PMLR, 2015, pp. 1530–1538.
- [34] A. Gupta, J. Johnson, L. Fei-Fei, S. Savarese, and A. Alahi, "Social gan: Socially acceptable trajectories with generative adversarial networks," in *Proceedings of the IEEE conference on computer vision and pattern recognition*, 2018, pp. 2255–2264.
- [35] N. Lee, W. Choi, P. Vernaza, C. B. Choy, P. H. Torr, and M. Chandraker, "Desire: Distant future prediction in dynamic scenes with interacting agents," in *Proceedings of the IEEE conference on computer vision and pattern recognition*, 2017, pp. 336–345.
- [36] N. Rhinehart, R. McAllister, K. Kitani, and S. Levine, "Precog: Prediction conditioned on goals in visual multi-agent settings," in *Proceedings of the IEEE/CVF International Conference on Computer Vision*, 2019, pp. 2821–2830.
- [37] H. Cheng, W. Liao, X. Tang, M. Y. Yang, M. Sester, and B. Rosenhahn, "Exploring dynamic context for multi-path trajectory prediction," in *2021 IEEE International Conference on Robotics and Automation (ICRA)*. IEEE, 2021, pp. 12 795–12 801.
- [38] M. Lee, S. S. Sohn, S. Moon, S. Yoon, M. Kapadia, and V. Pavlovic, "Muse-vae: Multi-scale vae for environment-aware long term trajectory prediction," in *Proceedings of the IEEE/CVF Conference on Computer Vision and Pattern Recognition*, 2022, pp. 2221–2230.
- [39] Y. Chen, B. Ivanovic, and M. Pavone, "Scept: Scene-consistent, policy-based trajectory predictions for planning," in *Proceedings of the IEEE/CVF Conference on Computer Vision and Pattern Recognition*, 2022, pp. 17 103–17 112.
- [40] T. Salzmann, B. Ivanovic, P. Chakravarty, and M. Pavone, "Trajectron++: Dynamically-feasible trajectory forecasting with heterogeneous data," in *European Conference on Computer Vision*. Springer, 2020, pp. 683–700.

- [41] B. Varadarajan, A. Hefny, A. Srivastava, K. S. Refaat, N. Nayakanti, A. Cornman, K. Chen, B. Douillard, C. P. Lam, D. Anguelov *et al.*, “Multipath++: Efficient information fusion and trajectory aggregation for behavior prediction,” in *2022 International Conference on Robotics and Automation (ICRA)*. IEEE, 2022, pp. 7814–7821.
- [42] N. Deo, E. Wolff, and O. Beijbom, “Multimodal trajectory prediction conditioned on lane-graph traversals,” in *Conference on Robot Learning*. PMLR, 2022, pp. 203–212.
- [43] E. Richardson and Y. Weiss, “On gans and gmms,” *Advances in Neural Information Processing Systems*, vol. 31, 2018.
- [44] H. Cui, V. Radosavljevic, F.-C. Chou, T.-H. Lin, T. Nguyen, T.-K. Huang, J. Schneider, and N. Djuric, “Multimodal trajectory predictions for autonomous driving using deep convolutional networks,” in *2019 International Conference on Robotics and Automation (ICRA)*. IEEE, 2019, pp. 2090–2096.
- [45] Y. Yuan and K. Kitani, “Dlow: Diversifying latent flows for diverse human motion prediction,” in *European Conference on Computer Vision*. Springer, 2020, pp. 346–364.
- [46] Y. J. Ma, J. P. Inala, D. Jayaraman, and O. Bastani, “Likelihood-based diverse sampling for trajectory forecasting,” in *Proceedings of the IEEE/CVF International Conference on Computer Vision*, 2021, pp. 13 279–13 288.
- [47] C. Yu, X. Ma, J. Ren, H. Zhao, and S. Yi, “Spatio-temporal graph transformer networks for pedestrian trajectory prediction,” in *European Conference on Computer Vision*. Springer, 2020, pp. 507–523.
- [48] Y. Chai, B. Sapp, M. Bansal, and D. Anguelov, “Multipath: Multiple probabilistic anchor trajectory hypotheses for behavior prediction,” in *Proceedings of the Conference on Robot Learning*, ser. Proceedings of Machine Learning Research, L. P. Kaelbling, D. Kragic, and K. Sugiura, Eds., vol. 100. PMLR, 30 Oct–01 Nov 2020, pp. 86–99.
- [49] J. Sun, Y. Li, H.-S. Fang, and C. Lu, “Three steps to multimodal trajectory prediction: Modality clustering, classification and synthesis,” in *Proceedings of the IEEE/CVF International Conference on Computer Vision*, 2021, pp. 13 250–13 259.
- [50] B. Pang, T. Zhao, X. Xie, and Y. N. Wu, “Trajectory prediction with latent belief energy-based model,” in *Proceedings of the IEEE/CVF Conference on Computer Vision and Pattern Recognition*, 2021, pp. 11 814–11 824.
- [51] D. P. Kingma and J. Ba, “Adam: A method for stochastic optimization,” in *Proceedings of the 3rd International Conference for Learning Representations*, 2015.
- [52] T. Salzmann, B. Ivanovic, P. Chakravarty, and M. Pavone, “Trajectron++,” 2020. [Online]. Available: <https://github.com/StanfordASL/Trajectron-plus-plus/issues/53>
- [53] Y. Yuan, X. Weng, Y. Ou, and K. M. Kitani, “Agentformer,” 2021. [Online]. Available: <https://github.com/Khrylx/AgentFormer/issues/5>